

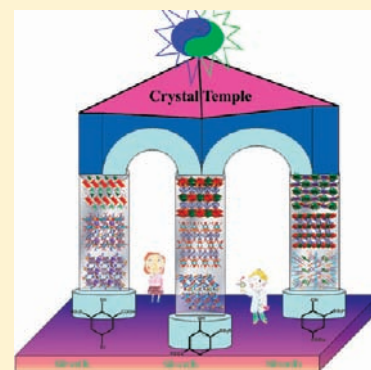
New Family of Silver(I) Complexes Based on Hydroxyl and Carboxyl Groups Decorated Arenesulfonic Acid: Syntheses, Structures, and Luminescent Properties

Xiang-Qian Fang, Zhao-Peng Deng, Li-Hua Huo, Wang Wan, Zhi-Biao Zhu,* Hui Zhao, and Shan Gao*

Key Laboratory of Functional Inorganic Material Chemistry, Ministry of Education, Heilongjiang University, Harbin 150080, People's Republic of China

Supporting Information

ABSTRACT: Self-assembly of silver(I) salts and three *ortho*-hydroxyl and carboxyl groups decorated arenesulfonic acids affords the formation of nine silver(I)-sulfonates, $(\text{NH}_4)\cdot[\text{Ag}(\text{HL1})(\text{NH}_3)(\text{H}_2\text{O})]$ (1), $\{(\text{NH}_4)\cdot[\text{Ag}_3(\text{HL1})_2(\text{NH}_3)(\text{H}_2\text{O})]\}_n$ (2), $[\text{Ag}_2(\text{HL1})(\text{H}_2\text{O})_2]_n$ (3), $[\text{Ag}_2(\text{HL2})(\text{NH}_3)_2]\cdot\text{H}_2\text{O}$ (4), $[\text{Ag}(\text{H}_2\text{L2})(\text{H}_2\text{O})]_n$ (5), $[\text{Ag}_2(\text{HL2})]_n$ (6), $[\text{Ag}_3(\text{L3})(\text{NH}_3)_3]_n$ (7), $[\text{Ag}_2(\text{HL3})]_n$ (8), and $[\text{Ag}_6(\text{L3})_2(\text{H}_2\text{O})_3]_n$ (9) ($\text{H}_3\text{L1}$ = 2-hydroxyl-3-carboxyl-5-bromobenzenesulfonic acid, $\text{H}_3\text{L2}$ = 2-hydroxyl-4-carboxylbenzenesulfonic acid, $\text{H}_3\text{L3}$ = 2-hydroxyl-5-carboxylbenzenesulfonic acid), which are characterized by elemental analysis, IR, TGA, PL, and single-crystal X-ray diffraction. Complex 1 is 3-D supramolecular network extended by $[\text{Ag}(\text{HL1})(\text{NH}_3)(\text{H}_2\text{O})]^-$ anions and NH_4^+ cations. Complex 2 exhibits 3-D host-guest framework which encapsulates ammonium cations as guests. Complex 3 presents 2-D layer structure constructed from 1-D tape of sulfonate-bridged Ag1 dimers linked by $[(\text{Ag}_2)_2(\text{COO})_2]$ binuclear units. Complex 4 exhibits 3-D hydrogen-bonding host-guest network which encapsulates water molecules as guests. Complex 5 shows 3-D hybrid framework constructed from organic linker bridged 1-D Ag-O-S chains while complex 6 is 3-D pillared layered framework with the inorganic substructure constructing from the Ag2 polyhedral chains interlinked by Ag1 dimers and sulfonate tetrahedra. The hybrid 3-D framework of complex 7 is formed by L3^- trianions bridging short trisilver(I) sticks and silver(I) chains. Complex 8 also presents 3-D pillared layered framework, and the inorganic layer substructure is formed by the sulfonate tetrahedrons bridging $[(\text{Ag1O}_4)_2(\text{Ag2O}_5)_2]_\infty$ motifs. Complex 9 represents the first silver-based metal-polyhedral framework containing four kinds of coordination spheres with low coordination numbers. The structural diversities and evolutions can be attributed to the synthetic methods, different ligands and coordination modes of the three functional groups, that is, sulfonate, hydroxyl and carboxyl groups. The luminescent properties of the nine complexes have also been investigated at room temperature, especially, complex 1 presents excellent blue luminescence and can sensitize Tb(III) ion to exhibit characteristic green emission.



INTRODUCTION

Design and synthesis of silver(I)-sulfonates have been an active research field in crystal engineering and coordination chemistry¹⁻⁷ in view of their potential applications in the area of intercalation chemistry, photochemistry, and porous materials and fascinating structural diversities arising from the versatile coordination geometries of Ag(I) ion⁸ and diversiform bridging modes of sulfonate (RSO_3^-).⁹ Actually, the sulfonate group is considered to be a weak ligand which is often evidenced by its inability to replace solvent molecules from the coordination spheres of many metal ions, and in many cases it is only involved in hydrogen bonding supramolecular networks.¹⁰ In order to modulate the binding modes and the topological architectures of silver(I)-sulfonates, neutral N-containing secondary ligands are employed, and many such mixed-ligand silver(I)-sulfonates have been reported based on Cambridge Structural Database CSD research (version 5.27).¹¹ However, the structures are highly dependent on the presence of N-containing secondary ligands, whereas the sulfonates serve as either noncoordinating counteranions or

simple coordination modes.¹ By contrast, only around 39 of the 186 crystallographically characterized silver(I)-sulfonates¹¹ are constructed from pure arenesulfonic acids. Significantly, although these 39 complexes feature alluring 0-D separated,^{1d,2} 1-D columnar,^{1g,3} 2-D layered,^{1e,4} and 3-D pillared layered⁵ silver(I)-sulfonate frameworks with prominent properties of fluorescent properties,^{1e,4e} as well as intriguing selective and reversible guest inclusion,^{4d} the influence of the nature of arenesulfonic acids on the solid structures and properties of silver(I) complexes are relatively uncommon. Hence, it is still a tempting challenge to synthesis silver(I)-sulfonates with attractive structures and properties through the rational design of pure arenesulfonic acids.

In this sense, decoration of arenesulfonic acids by attaching additional functional groups such as carboxyl, hydroxyl, and amine groups is another effective way to improve the coordination abilities of sulfonate ligands.^{1e,g,4i} In our previous

Received: July 24, 2011

Published: November 16, 2011

studies, we have demonstrate that the introduction of hydroxyl groups at the *ortho*-position can effectively enrich the coordination modes of the $-\text{SO}_3$ group and modulate the final topological structures of silver(I)-sulfonates.⁷ Moreover, 5-sulfosalicylic acid (H_3SSA), a simple but interesting ligand with three potential coordinating groups of $-\text{OH}$, $-\text{CO}_2\text{H}$, and $-\text{SO}_3\text{H}$, can easily coordinate to metal ions with different modes and lead to the formation of high-dimensional architectures.^{4e,f,5a} Consequently, three successors of H_3SSA , namely, 2-hydroxyl-3-carboxyl-5-bromobenzenesulfonic acid ($\text{H}_3\text{L1}$), 2-hydroxyl-4-carboxylbenzenesulfonic acid ($\text{H}_3\text{L2}$), and 2-hydroxyl-5-carboxylbenzenesulfonic acid ($\text{H}_3\text{L3}$), have been designed and exploited to construct novel topological structures with excellent properties considering the following

points. (a) As versatile tectons, the three ligands contain the same multifunctional groups, which may be partially or completely deprotonated and normally serve as bridging connector to construct diverse supramolecular aggregations or coordination polymers via different coordination and/or intermolecular forces. (b) In comparison with the *para*-position of hydroxyl group in H_3SSA , the hydroxyl groups at the *ortho*-position of sulfonate groups can effectively enrich the coordination modes and binding abilities of the $-\text{SO}_3$ group to modify the topological structures of silver(I)-sulfonates. (c) The carboxyl group binds to $\text{Ag}(\text{I})$ ion in a variety of coordination modes and thus affords the argentophilic interactions, which have been proved to be one of the most important factors contributing to the formation of $\text{Ag}(\text{I})$

Table 1. Crystal Data and Structure Refinement Parameters of Complexes 1–9

	1	2	3	4	
empirical formula	$\text{C}_7\text{H}_{12}\text{N}_2\text{O}_7\text{SBrAg}$	$\text{C}_{14}\text{H}_{15}\text{N}_2\text{O}_{13}\text{S}_2\text{Br}_2\text{Ag}_3$	$\text{C}_7\text{H}_7\text{O}_8\text{SBrAg}_2$	$\text{C}_{14}\text{H}_{24}\text{N}_4\text{O}_{14}\text{S}_2\text{Ag}_4$	
M_r	456.03	966.83	546.84	967.97	
cryst syst	triclinic	triclinic	triclinic	monoclinic	
space group	$P\bar{1}$	$P\bar{1}$	$P\bar{1}$	$P2_1/c$	
$a/\text{\AA}$	7.5987(15)	9.4697(19)	6.6639(13)	13.257(3)	
$b/\text{\AA}$	9.4869(19)	10.256(2)	9.5487(19)	6.5426(13)	
$c/\text{\AA}$	9.5920(19)	12.099(2)	9.977(2)	14.635(3)	
α/deg	93.83(3)	87.90(3)	84.26(3)	90.00	
β/deg	105.80(3)	88.38(3)	75.75(3)	104.98(3)	
γ/deg	94.93(3)	81.24(3)	86.71(3)	90.00	
$V/\text{\AA}^3$	660.0(2)	1160.3(4)	611.9(2)	1226.2(4)	
Z	2	2	2	2	
$D_c/\text{mg m}^{-3}$	2.295	2.767	2.968	2.622	
μ/mm^{-1}	4.742	6.201	6.667	3.395	
θ range	3.05–27.46	3.15–25.00	3.14–27.45	3.18–27.47	
reflns collected	6455	9165	6029	11 225	
unique reflns	2973	4076	2769	2803	
no. of params	184	343	178	179	
$F(000)$	444	920	516	936	
$R1, wR2 [I > 2\sigma(I)]$	0.0576, 0.1561	0.0361, 0.0999	0.0469, 0.1141	0.0727, 0.1799	
GOF on F^2	1.073	1.090	1.017	1.036	
largest and hole/ $e\cdot\text{\AA}^{-3}$	1.644, -1.329	1.919, -1.128	1.987, -1.317	1.612, -1.596	
complex	5	6	7	8	9
empirical formula	$\text{C}_7\text{H}_7\text{O}_7\text{SAg}$	$\text{C}_7\text{H}_4\text{O}_6\text{SAg}_2$	$\text{C}_7\text{H}_{12}\text{N}_3\text{O}_6\text{SAg}_3$	$\text{C}_7\text{H}_4\text{O}_6\text{SAg}_2$	$\text{C}_{14}\text{H}_{12}\text{O}_{15}\text{S}_2\text{Ag}_6$
M_r	343.06	431.90	589.87	431.90	1131.58
cryst syst	monoclinic	monoclinic	triclinic	triclinic	monoclinic
space group	$C2/c$	$C2/c$	$P\bar{1}$	$P\bar{1}$	$P2_1/c$
$a/\text{\AA}$	20.417(4)	19.227(4)	6.2647(13)	6.9889(14)	10.8102(4)
$b/\text{\AA}$	7.7642(16)	8.2824(17)	8.3431(17)	7.4711(15)	16.2514(5)
$c/\text{\AA}$	11.886(2)	11.582(2)	12.831(3)	9.6405(19)	12.5666(4)
α/deg	90.00	90.00	89.65(3)	70.80(3)	90.00
β/deg	103.96(3)	106.27(3)	80.19(3)	85.46(3)	94.5590(10)
γ/deg	90.00	90.00	83.36(3)	73.85(3)	90.00
$V/\text{\AA}^3$	1828.6(6)	1770.5(6)	656.4(2)	456.6(2)	2200.73(13)
Z	8	8	2	2	4
$D_c/\text{mg m}^{-3}$	2.492	3.241	2.985	3.142	3.415
μ/mm^{-1}	2.452	4.668	4.618	4.525	5.504
θ range	3.19–27.45	3.71–27.46	3.22–27.48	3.00–27.44	3.14–27.46
reflns collected	8627	6565	6397	4502	21 060
unique reflns	2083	2021	2963	2062	5014
no. of params	154	145	184	148	358
$F(000)$	1344	1632	560	408	2120
$R1, wR2 [I > 2\sigma(I)]$	0.0216, 0.0455	0.0446, 0.0875	0.0514, 0.1493	0.0310, 0.0758	0.0479, 0.1162
GOF on F^2	1.094	1.005	1.051	1.086	1.071
largest and hole/ $e\cdot\text{\AA}^{-3}$	0.719, -0.678	0.880, -0.778	1.596, -1.816	1.573, -0.916	2.217, -1.221

complexes and special properties.^{1e,12} As part of our long-term ongoing research on the coordination chemistry of silver(I)–sulfonates, we presented in this article the syntheses, structures and luminescent properties of nine new complexes based on the above three ligands and different silver(I) salts, namely, $(\text{NH}_4)\cdot[\text{Ag}(\text{HL1})(\text{NH}_3)(\text{H}_2\text{O})]$ (**1**), $\{(\text{NH}_4)\cdot[\text{Ag}_3(\text{HL1})_2(\text{NH}_3)(\text{H}_2\text{O})]\}_n$ (**2**), $[\text{Ag}_2(\text{HL1})(\text{H}_2\text{O})_2]_n$ (**3**), $[\text{Ag}_2(\text{HL2})(\text{NH}_3)_2]\cdot\text{H}_2\text{O}$ (**4**), $[\text{Ag}(\text{H}_2\text{L2})(\text{H}_2\text{O})]_n$ (**5**), $[\text{Ag}_2(\text{HL2})]_n$ (**6**), $[\text{Ag}_3(\text{L3})(\text{NH}_3)_3]_n$ (**7**), $[\text{Ag}_2(\text{HL3})]_n$ (**8**), and $[\text{Ag}_6(\text{L3})_2(\text{H}_2\text{O})_3]_n$ (**9**). Complexes **1** and **4** exhibit host–guest 3-D supramolecular networks extended by the N/O–H...O hydrogen bonds. Complex **3** presents 2-D layer structure constructed from 1-D tape of sulfonate-bridged AgI dimers linked by $[(\text{Ag}_2)_2(\text{COO})_2]$ binuclear units. Complexes **2** and **5–9** exhibit 3-D host–guest, hybrid and pillared layered frameworks, respectively. The structural diversities and evolutions can be attributed to the synthetic methods, coordination modes and different arenesulfonic acid ligands decorated by hydroxyl and carboxyl groups. Luminescent investigations indicate that complexes **1–3** and **5** exhibit strong blue emissions at room temperature. Moreover, complex **1** can sensitize Tb(III) ion to exhibit characteristic green emission at room temperature in aqueous solution.

EXPERIMENTAL SECTION

General Procedures. All chemicals and solvents were of A. R. grade and used without further purification for the syntheses. Elemental analyses were carried out with a Vario MICRO from Elementar Analysensysteme GmbH, and the infrared spectra (IR) were recorded from KBr pellets in the range of 4000–400 cm^{-1} on a Bruker Equinox 55 FT-IR spectrometer. Thermogravimetric analysis (TGA) were performed on a Perkin-Elmer TG/DTA 6300 thermal analyzer under flowing N_2 atmosphere, with a heating rate of 10 $^\circ\text{C}/\text{min}$. Luminescence spectra were measured on a Perkin-Elmer LS 55 luminance meter. To examine the possibility of modification of the luminescent properties through cation exchange, the solid sample of complex **1** was immersed in aqueous solution (1×10^{-4} $\text{mol}\cdot\text{L}^{-1}$) containing the same amount of Eu^{3+} and Tb^{3+} ions, respectively.

Syntheses of Ligands. 5-Bromo-2-hydroxybenzoic acid, 3-hydroxybenzoic acid, and 4-hydroxybenzoic acid were slowly added to different amounts of 20% oleum with stirring, respectively. The mixture was left to react 3 h at 120 $^\circ\text{C}$ and then cooled to room temperature. The laurel-green solids for $\text{H}_3\text{L2}$ and white solids for $\text{H}_3\text{L1}$ and $\text{H}_3\text{L3}$ were separated and recrystallized from hot water (Figure S1 in Supporting Information). $\text{H}_3\text{L1}$: yield 80%; mp 143–145 $^\circ\text{C}$. Elemental analysis calcd (%) for $\text{C}_7\text{H}_5\text{O}_6\text{BrS}$: C 28.30, H 1.70; found C 28.34, H 1.75. IR (ν/cm^{-1}): 3413s, 3235m, 3043w, 1666s, 1617s, 1589s, 1527m, 1459m, 1378m, 1357m, 1309m, 1238m, 1191w, 1039w, 989w, 952m, 821m, 692m, 611m, 516m. $\text{H}_3\text{L2}$: yield 82%; mp 230–232 $^\circ\text{C}$. Elemental analysis calcd (%) for $\text{C}_7\text{H}_6\text{O}_6\text{S}$: C 38.54, H 2.77; found C 38.59, H 2.83. IR (ν/cm^{-1}): 3274m,br, 3068w, 1698s, 1589 m, 1508 m, 1417s, 1374m, 1295m, 1220s, 1193s, 1149m, 1083m, 1018s, 948m, 883m, 759m, 703m, 634m, 561m, 524m. For $\text{H}_3\text{L3}$: yield 85%; mp 242–244 $^\circ\text{C}$. Elemental analysis calcd (%) for $\text{C}_7\text{H}_6\text{O}_6\text{S}$: C 38.54, H 2.77; found C 38.50, H 2.82. IR (ν/cm^{-1}): 3234m,br, 3060w, 1685s, 1602s, 1508 m, 1407s, 1363w, 1290s, 1203m, 1155m, 1079m, 1018m, 919w, 887m, 846m, 769m, 728m, 626m, 578m.

Synthesis of $(\text{NH}_4)\cdot[\text{Ag}(\text{HL1})(\text{NH}_3)(\text{H}_2\text{O})]$ (1**).** AgNO_3 (0.255 g, 1.5 mmol) and $\text{H}_3\text{L1}$ (0.149 g, 0.5 mmol) were mixed in 10 mL aqueous solution, and then the pH value was adjusted to ~ 6 with proper amount of ammonia. The mixture stirred at room temperature for 5 min followed by filtration. Colorless crystals of **1** were isolated from the filtrate after avoiding illumination for several days. Yield: 49% (based on Ag). Anal. Calcd for $\text{C}_7\text{H}_{12}\text{N}_2\text{O}_7\text{SBrAg}$: C 18.44, H 2.65, N 6.14%; found C 18.48, H 2.70, N 6.10%. IR (ν/cm^{-1}): 3423m, 3358s,

3278m, 3187s, 3073w, 1617m, 1581m, 1565m, 1425s, 1369m, 1267m, 1222m, 1191s, 1037s, 892m, 846m, 800m, 698m, 620s, 539m.

Synthesis of $\{(\text{NH}_4)\cdot[\text{Ag}_3(\text{HL1})_2(\text{NH}_3)(\text{H}_2\text{O})]\}_n$ (2**).** A similar procedure with complex **1** was carried out. The pH value was adjusted to ~ 7 with proper amount of ammonia. Pale-yellow crystals of **2** suitable for X-ray diffraction were isolated from the filtrate after avoiding illumination for several days. Yield: 58% (based on Ag). Anal. Calcd for $\text{C}_{14}\text{H}_{15}\text{N}_2\text{O}_{13}\text{S}_2\text{Br}_2\text{Ag}_3$: C 17.39, H 1.56, N 2.90%; found C 17.43, H 1.52, N 2.93%. IR (ν/cm^{-1}): 3439m, 3363m, 3178m, 3064w, 1614m, 1571m, 1427s, 1363m, 1268m, 1226m, 1157s, 1027s, 894m, 844m, 798m, 698m, 615s, 541m.

Synthesis of $[\text{Ag}_2(\text{HL1})(\text{H}_2\text{O})_2]_n$ (3**).** An aqueous solution of $\text{H}_3\text{L1}$ (0.298 g, 1.0 mmol) was added to an aqueous suspension containing Ag_2CO_3 (0.276 g, 1.0 mmol). The mixture was stirred for 40 min until no further CO_2 was given off, and then filtered. The resulting clear solution was allowed to evaporate slowly at room temperature after avoiding illumination for two weeks, and pale-yellow crystals of **3** suitable for X-ray diffraction were isolated. Yield: 53% (based on Ag).

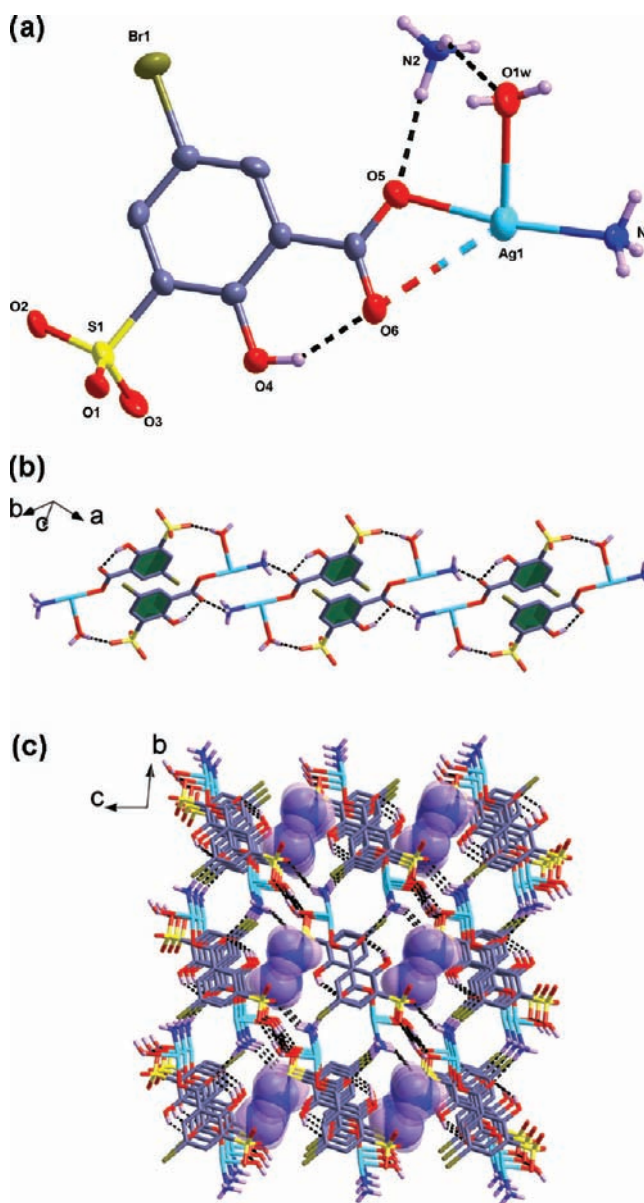


Figure 1. (a) Molecular structure of **1** with the ellipsoids drawn at the 50% probability level; the weak Ag–O interaction and hydrogen bonds are denoted by dash line. (b) 1-D chain structure containing dinuclear motifs. (c) 3-D supramolecular framework of **1**.

Anal. Calcd for $C_7H_7O_8SBrAg_2$: C 15.38, H 1.29%; found C 15.35, H 1.34%. IR (ν/cm^{-1}): 3440s (br), 3070w, 1612m, 1563m, 1427s, 1365m, 1268m, 1203s, 1168s, 1029s, 896m, 846m, 796w, 700m, 615s, 538m.

Synthesis of $[Ag_2(HL2)(NH_3)_2] \cdot H_2O$ (4). A similar procedure with complex 1 was carried out by changing H_3L1 into H_3L2 . Colorless crystals of 4 were isolated from the filtrate after avoiding illumination for several days. Yield: 62% (based on Ag). Anal. Calcd for $C_7H_{12}N_2O_7SAg_2$: C 17.37, H 2.50, N 5.79%; found C 17.34, H 2.45, N 5.82%. IR (ν/cm^{-1}): 3434m, 3340s, 3264m, 3056w, 1616m, 1592m, 1562s, 1409s, 1276m, 1251s, 1218s, 1184s, 1132m, 1076m, 1018s, 956m, 887m, 848w, 806m, 769m, 711m, 646s, 538m.

Synthesis of $[Ag(H_2L2)(H_2O)]_n$ (5). A similar procedure with complex 3 was carried out by changing H_3L1 into H_3L2 , and the mixture was stirred for 10 min. Colorless crystals of 5 were isolated from the filtrate after avoiding illumination for several days. Yield: 69% (based on Ag). Anal. Calcd for $C_7H_7O_7SAg$: C 24.51, H 2.06; found C 24.48, H 2.10. IR (ν/cm^{-1}): 3410m, 3246m, 3059w, 1688s, 1609m, 1587m, 1504m, 1416s, 1365m, 1313s, 1217s, 1119s, 1080s, 1011s, 941m, 888m, 763m, 708s, 639m, 568m, 530m.

Synthesis of $[Ag_2(HL2)]_n$ (6). A similar procedure with complex 5 was carried out by changing the ration of metal to ligand into 1.5:1, and the mixture was stirred for 20 min. Colorless crystals of 6 suitable for X-ray diffraction were isolated. Yield: 71% (based on Ag). Anal. Calcd for $C_7H_4O_6SAg_2$: C 19.47, H 0.93; found C 19.51, H 0.88. IR (ν/cm^{-1}): 3440m, 3058w, 1606m, 1544s, 1413s, 1332s, 1253m, 1193s,

1153s, 1132s, 1079s, 1010s, 943m, 881m, 773m, 711m, 634m, 565m, 545m.

Synthesis of $[Ag_3(L3)(NH_3)_3]_n$ (7). A similar procedure with complex 1 was carried out. The pH value was adjusted to ~ 8 with proper amount of ammonia, and pale-yellow crystals of 7 suitable for X-ray diffraction were isolated from the filtrate after avoiding illumination for several days. Yield: 44% (based on Ag). Anal. Calcd for $C_7H_{12}N_3O_6SAg_3$: C 14.25, H 2.05, N 7.12%; found C 14.28, H 2.01, N 7.15%. IR (ν/cm^{-1}): 3334m, 3289m, 3220m, 3053w, 1583m, 1558m, 1477m, 1371s, 1311m, 1230w, 1176s, 1124m, 1066s, 1016s, 894w, 831w, 802w, 777m, 730m, 646s, 574w, 528m.

Synthesis of $[Ag_2(HL3)]_n$ (8). A similar procedure with complex 3 was carried out by changing H_3L1 into H_3L3 . Colorless crystals of 8 suitable for X-ray diffraction were isolated. Yield: 61% (based on Ag). Anal. Calcd for $C_7H_4O_6SAg_2$: C 19.47, H 0.93%; found C 19.45, H 0.89%. IR (ν/cm^{-1}): 3440m, 3058w, 1606m, 1558s, 1479m, 1372s, 1310m, 1243m, 1182s, 1130s, 1070s, 1022s, 898w, 810w, 782m, 743m, 651m, 541m.

Synthesis of $[Ag_6(L3)_2(H_2O)_3]_n$ (9). A similar procedure with complex 8 was carried out by changing the ration of metal to ligand into 2:1, and pale-yellow crystals of 9 suitable for X-ray diffraction were isolated. Yield: 67% (based on Ag). Anal. Calcd for $C_{14}H_{12}O_{15}S_2Ag_6$: C 14.86, H 1.07%; found C 14.83, H 1.09%. IR (ν/cm^{-1}): 3342m (br), 3045w, 1597m, 1560s, 1481m, 1369s, 1311m, 1241m, 1178s, 1128s, 1068m, 1020m, 894w, 844w, 802m, 775m, 730m, 646s, 576w, 539m.

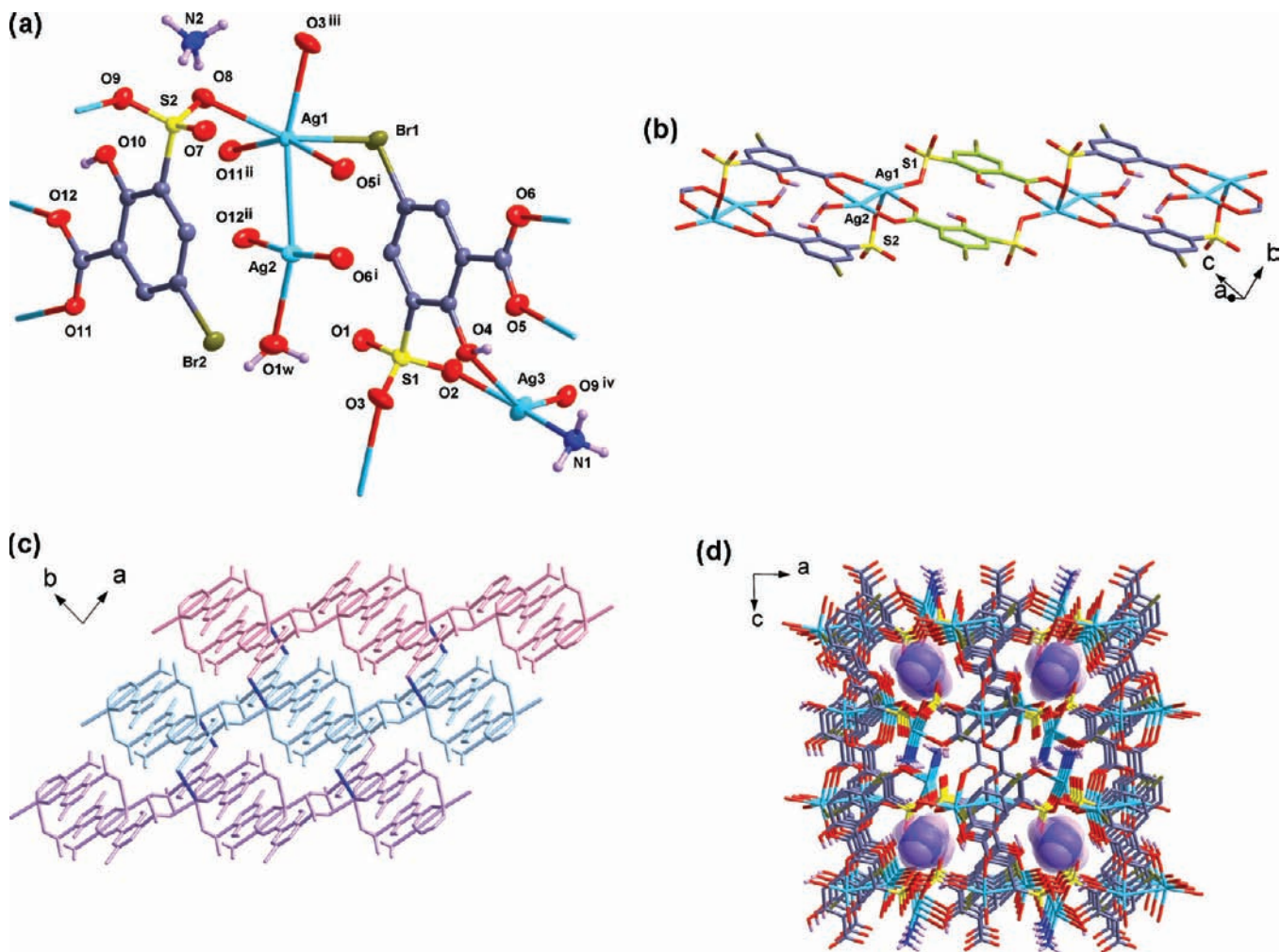


Figure 2. (a) Perspective view of the asymmetric unit of 2 showing the coordination environments around the silver centers with the ellipsoids drawn at the 50% probability level. (b) 1-D double chain structure with the carbon atoms of S1-containing dianions denoted as lime sticks. (c) 2-D layer structure extended by the Ag–Br interactions (blue bonds) linking adjacent chains. (d) 3-D Host–guest framework with the ammonium cations encapsulated in the channels.

X-ray Crystallographic Measurements. Table 1 provides a summary of the crystal data, data collection, and refinement parameters for the complexes 1–9. All diffraction data were collected at 295 K on a RIGAKU RAXIS-RAPID diffractometer with graphite monochromatized Mo $K\alpha$ ($\lambda = 0.71073$ Å) radiation in ω scan mode. All structures were solved by direct method and difference Fourier syntheses. All non-hydrogen atoms were refined by full-matrix least-squares techniques on F^2 with anisotropic thermal parameters. The hydrogen atoms attached to carbon atoms were placed in calculated positions with $C-H = 0.93$ Å and $U(H) = 1.2U_{eq}(C)$ in the riding model approximation. The hydrogen atoms of hydroxyl groups in complexes 1–6, 8 and water molecules in complexes 1–5, 9 were placed in calculated positions and located in difference Fourier maps and refined in the riding model approximation, with O–H distances restraint (0.82 or 0.85(1) Å) and $U(H) = 1.5U_{eq}(O)$, respectively. Hydrogen atoms of ammonia molecules in complexes 1, 2, 4, and 7 were placed in calculated positions with $N-H = 0.89$ Å and $U(H) = 1.5U_{eq}(N)$, while the hydrogen atoms of ammonium cations in complexes 1 and 2 were located in difference Fourier maps and refined in the riding model approximation, with N–H distances restraint (0.86(1) or 0.89(1) Å) and $U(H) = 1.5U_{eq}(N)$. All calculations were carried out with the SHELXL97 program.¹³ The CCDC reference numbers are 836149–836156 and 798868 for complexes 1–9. Selected bond distances and angles and selected hydrogen bond parameters for all complexes are presented in Table S1 and Table S2, respectively (Supporting Information).

RESULTS AND DISCUSSION

Structure of $(NH_4)[Ag(HL1)(NH_3)(H_2O)]$ (1). Single-crystal X-ray diffraction analysis reveals that complex 1 presents 3-D supramolecular network extended by the N/O–H \cdots O hydrogen bonds. As illustrated in Figure 1a, the asymmetric unit consists of one ammonium cation and 0-D discrete structure of $[Ag(HL1)(NH_3)(H_2O)]^-$ anion. The coordination sphere of Ag(I) ion can be best described as T-shaped geometry with the long separation of 2.945(4) Å indicating the existence of weak Ag(I)–O6 interaction.¹⁴ The sulfonate groups in $HL1^{2-}$ dianions do not coordinate to Ag(I) and just direct toward water H atoms to form classic O–H \cdots O hydrogen bonds which link the mononuclear unit into dinuclear motif. Adjacent dinuclear motifs are further interconnected by the hydrogen bonds between coordinated ammonia molecules and carboxylate groups to form a 1-D chain structure, in which the $\pi\cdots\pi$ stacking interactions between the opposite phenyl rings are observed with the centroid-to-centroid distances of 3.627 Å (Figure 1b). Subsequently, the ammonium cations bridge the aforementioned chains into 3-D supramolecular network through N–H \cdots O hydrogen bonds (Figure 1c).

Structure of $\{(NH_4)[Ag_3(HL1)_2(NH_3)(H_2O)]\}_n$ (2). As illustrated in Figure 2a, the asymmetric unit of complex 2 contains three crystallographically unique Ag(I) ions, two $HL1^{2-}$ dianions, one coordinated ammonia molecule, one coordinated water molecule and one ammonium cation. Ag1 displays distorted trigonal bipyramid geometry while Ag2 exhibits T-shaped geometry. The coordination sphere of Ag3 can be described as twist quadrilateral geometry which is rarely observed in silver(I)-complexes (Figure S2 in Supporting Information). The O4 and O9^{iv} atoms locate on top of the N1/Ag3/O2 plane with the vertical distances being 0.556 and 0.859 Å. The two $HL1^{2-}$ dianions adopt different coordination modes and interlink adjacent Ag(I) ions to form the final 3-D hybrid framework, which can be understood in the following manners. First, as shown in Figure 2b, the S2-containing $HL1^{2-}$ dianions in the μ_1 (sulfonate): μ_2 (carboxylate) mode join Ag1

and Ag2 ions to generate tetranuclear motifs, which further connect by S1-containing $HL1^{2-}$ dianions in the same mode, thus forming 1-D double chain structure along the diagonal of *ac* plane. The short Ag1 \cdots Ag2 distance of 2.9033(9) Å indicates the existence of argentophilic interaction.¹⁵ Subsequently, the Br atoms of S1-containing $HL1^{2-}$ dianions coordinate to the Ag1 ions of adjacent chains and extend the chains into 2-D layer structure with the Ag–Br bond of 2.9978(10) Å falling in the reported range of 2.7–3.0 Å (Figure 2c).¹⁶ Finally, Ag3 ions join the 2-D layers through the coordination of sulfonate oxygen atoms (O2 and O9) and hydroxyl atoms (O4), thus giving rise to 3-D host–guest framework with the ammonium cations encapsulated in the channels (Figure 2d).

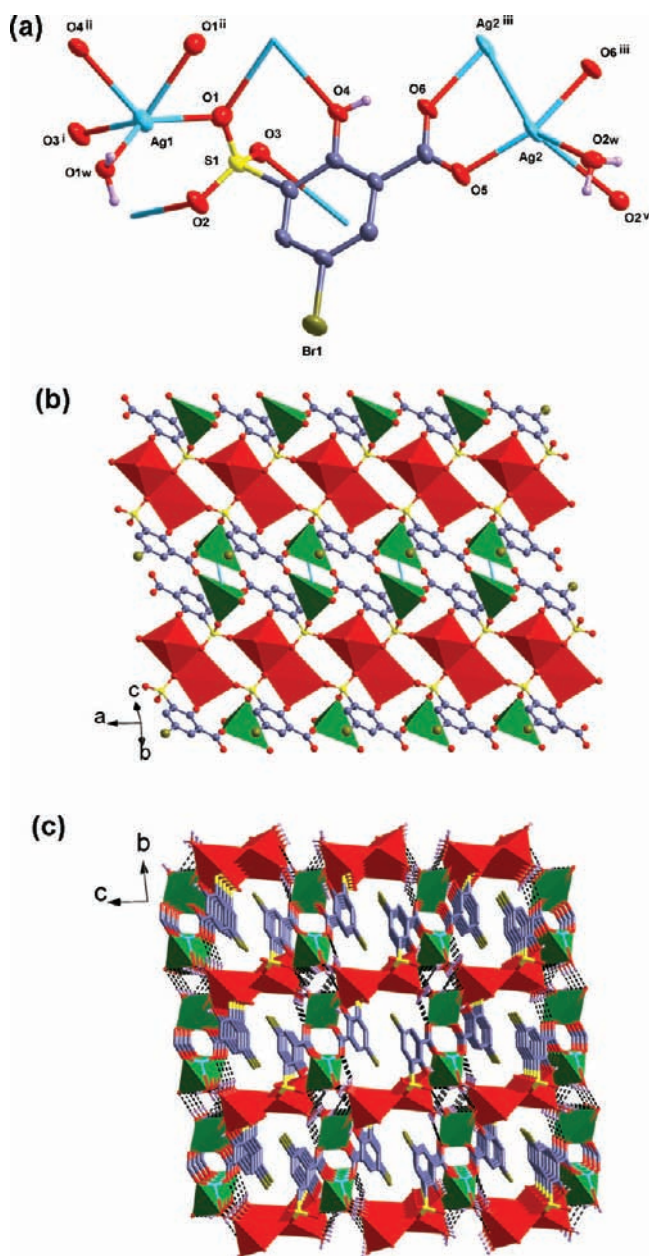


Figure 3. (a) Perspective view of the asymmetric unit of 3 showing the coordination environments around the silver centers with the ellipsoids drawn at the 50% probability level. (b) Representation of the 2-D layer (red polyhedra: Ag1; green polyhedra: Ag2; sky blue bonds: Ag \cdots Ag interactions). (c) Illustration of the 3-D network formed by the hydrogen bonds linking adjacent layers.

Structure of $[\text{Ag}_2(\text{HL1})(\text{H}_2\text{O})_2]_n$ (3). The asymmetric unit of complex 3 contains two crystallographically unique Ag(I) ions, one HL1^{2-} dianion and two coordinated water molecules, in which the two Ag(I) ions exhibit different coordinating geometries (Figure 3a). Ag1 exhibits distorted square-pyramidal geometry, while Ag2 can be best described as distorted tetrahedral geometry with the long contact of 2.931(5) Å (Ag2–O2) being considerably less than the sum of the van der Waals radii (3.24 Å). As shown in Figure 3b, two Ag1 ions are bridged by two symmetry-related O1 atoms of sulfonate groups and form binuclear units, which are further joined by the pairs of O3 atoms of sulfonate groups to generate a 1-D tape along the *a*-axis. Ag2 ions are fastened by the residual O2 atom of sulfonate group together with the carboxylate oxygen atoms and arranged along the two edges of the 1-D tape, which connect adjacent tapes into 2-D layer structure. Weak Ag⋯Ag interactions are observed between Ag2 ions with the separation of 3.0472(16) Å. Furthermore, the 3-D framework with regular channels is formed by the extensive hydrogen bonds involving the coordinated water molecules, sulfonate groups and carboxylate groups (Figure 3c). The 1-D channels are occupied by the coordinated HL1^{2-} dianions with the Br “tail” toward to the sulfonate groups. The shortest distance between Br and O atoms (3.066(6) Å) indicates the existence of weak Br⋯O interaction.

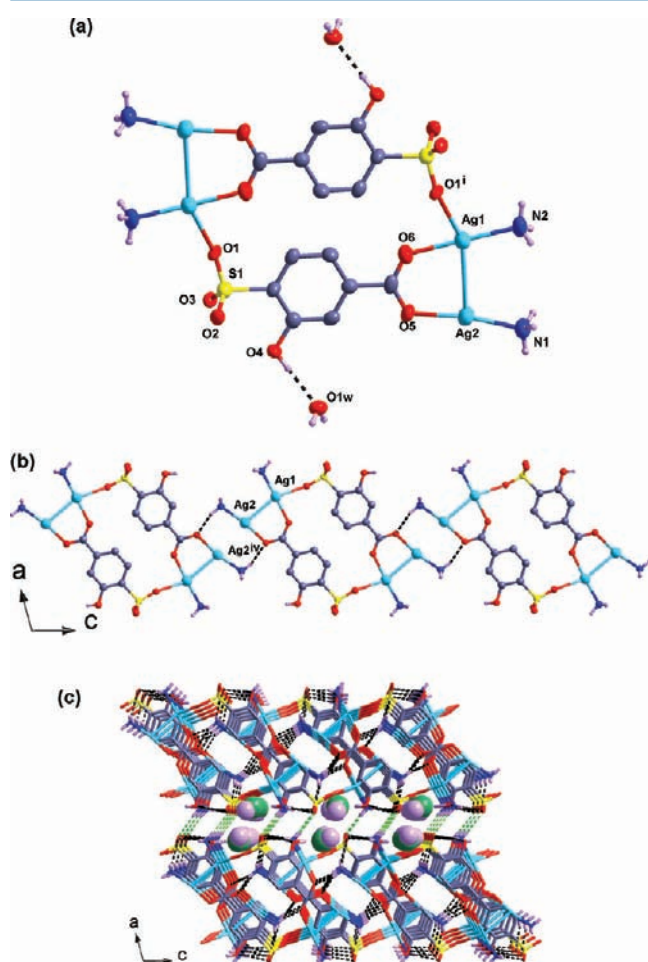


Figure 4. (a) Perspective view of the asymmetric unit of 4 showing the coordination environments around the silver center with the ellipsoids drawn at the 50% probability level. (b) Illustration of the hydrogen-bonding chain with the hydrogen bonds denoted by dash line. (c) 3-D supramolecular network with the water molecules encapsulated in the hydrogen-bonding channels.

Structure of $[\text{Ag}_2(\text{HL2})(\text{NH}_3)_2]\cdot\text{H}_2\text{O}$ (4). Single-crystal X-ray diffraction analysis reveals that complex 4 is 0-D discrete tetranuclear structure. The asymmetric unit contains two crystallographically unique Ag(I) ions, one HL2^{2-} dianion, two coordinated ammonia molecules and one free water molecule (Figure 4a). Ag1 exhibits T-shaped geometry, while Ag2 exhibits linear geometry. The two Ag(I) ions are bridged by the carboxylate group in a bridging mode to generate a dinuclear unit with the Ag⋯Ag separation of 2.9696(16) Å, which is further linked by two symmetry-related HL2^{2-} dianions through O1 atom into a tetranuclear motif. As shown in Figure 4b, adjacent tetranuclear motifs are interconnected through pairs of N(1)–H(1N1)⋯O(5) hydrogen bonds into 1-D chain incorporating $R_2^2(8)$ rings along the *c*-axis. The Ag⋯Ag distance of 3.4169(15) Å between the Ag2 ions in the ring indicates the weak Ag⋯Ag interaction, owing to the distance being slightly shorter than the summed van der Waals radii of two silver atoms (3.44 Å).¹⁵ Subsequently, various N/O–H⋯O hydrogen bonds between uncoordinated sulfonates, hydroxyl groups, coordinated carboxylates and ammonia molecules link adjacent chains into 3-D supramolecular network with the free water molecules encapsulated in the hydrogen-bonding channels (Figure 4c).

Structure of $[\text{Ag}(\text{H}_2\text{L2})(\text{H}_2\text{O})]_n$ (5). Complex 5 shows 3-D framework with the asymmetric unit composed of one Ag(I) ion, one $\text{H}_2\text{L2}^-$ monoanion and one coordinated water molecule (Figure 5a). The coordination sphere of Ag(I) ion

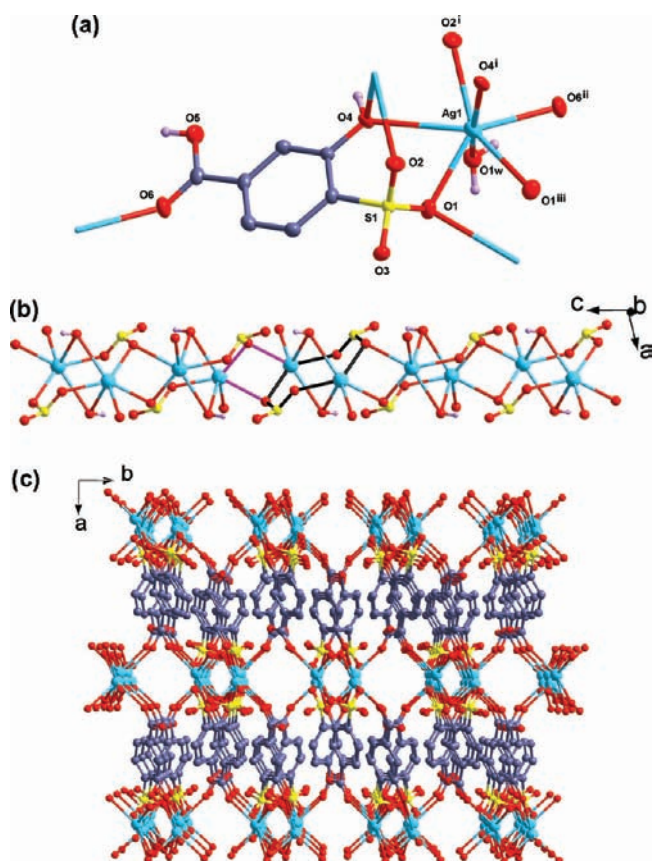


Figure 5. (a) Perspective view of the asymmetric unit of 5 showing the coordination environment around the silver center with the ellipsoids drawn at the 50% probability level. (b) Ball-and-stick representation of the Ag–O–S chain incorporating four-membered ring (pink) and eight-membered ring (black). (c) Illustration of the 3-D hybrid framework.

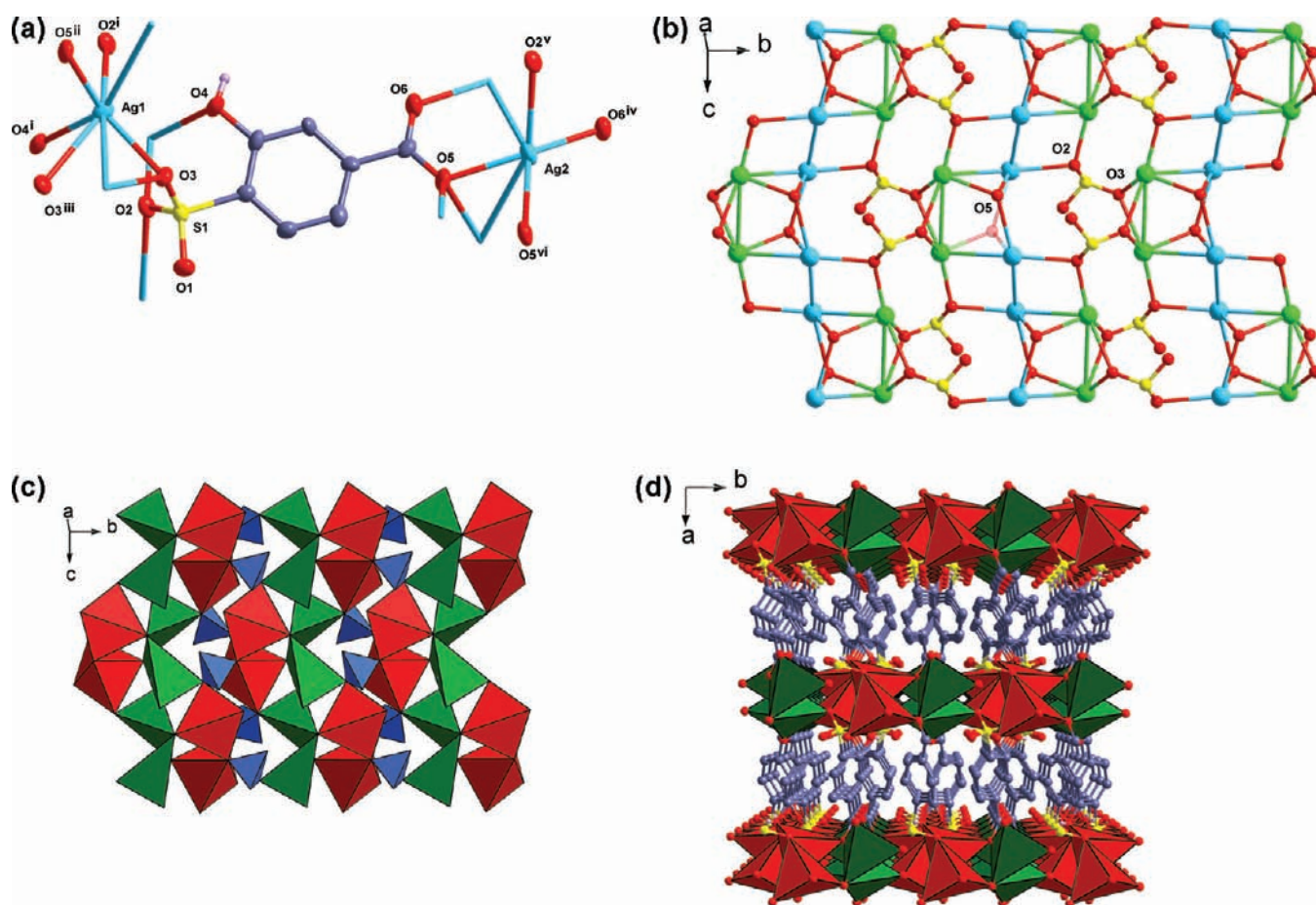


Figure 6. (a) Perspective view of the asymmetric unit of **6** showing the coordination environments around the silver centers with the ellipsoids drawn at the 50% probability level. (b) The Ag–O–S layer formed by the sulfonate groups linking silver chains (green balls, Ag1; sky blue balls, Ag2). (c) Polyhedral representation of the Ag–O–S layer (red polyhedra, Ag1; green polyhedra, Ag2; blue polyhedra: sulfonate group). (d) Illustration of the 3-D pillared layered structure.

can be described as distorted trigonal prism geometry with the longer separation of 2.917(2) Å (Ag1–O4) capped the lateral face. The sulfonate groups exhibit μ_3 ($\kappa^2\text{O}1$, $\kappa^1\text{O}2$) coordination mode and bridge adjacent Ag1 ions into 1-D chain structure along the *c*-axis which incorporates four-membered rings and eight-membered rings (Figure 5b). The Ag \cdots Ag distances of 3.6915(8) and 3.4867(6) Å in the two rings are longer than the summed van der Waals radii of two silver atoms (3.44 Å). Two hydroxyl groups cap each face of the eight-membered ring in a μ_2 mode. The carboxylate group acts in monodentate mode and coordinates to the above 1-D chain, thus leading to the formation of the 3-D hybrid framework (Figure 5c).

Structure of [Ag₂(HL2)]_n (6). Figure 6a presents the asymmetric unit of complex **6** which contains two crystallographically unique Ag(I) ions and one HL2²⁻ dianion. The coordination sphere about Ag1 is distorted trigonal bipyramid geometry, and even longer contacts to two adjacent Ag(I) ions (Ag1 \cdots Ag2ⁱⁱⁱ 3.0745(9) Å, Ag1 \cdots Ag1ⁱⁱⁱ 3.3931(10) Å), while Ag2 has distorted tetrahedron geometry and connects to one Ag1 ion with the previously quoted distances and one Ag2 ion with the distance of 2.9671(16) Å. It should be noted that adjacent Ag(I) ions are connected into 1-D concave-convex chain along the *c*-axis through the aforementioned Ag \cdots Ag interactions. The sulfonate group acts in μ_4 ($\kappa^2\text{O}2$, $\kappa^2\text{O}3$) coordination mode and bridges the concave-convex silver chains into 2-D layer

structure (Figure 6b). A pair of carboxylate OS atoms caps each face of the Ag₄ core in an unusual μ_3 mode. Instead, the 2-D layer can be described as the edge-sharing Ag1 dimers modified Ag2 polyhedral chain interlinked by the tetrahedron of the sulfonate (CSO₃) (Figure 6c). Figure 6d exhibits the 3-D pillared layered framework of complex **6**, in which the phenyl rings act as the pillars. The interlayer distance, defined as the perpendicular distance between planes of Ag(I) ions, is 9.23 Å, and the thickness of a single lamella, defined as the region containing solely the Ag, S, and O atoms, is 3.63 Å. Thus, the gallery height present in complex **6** is 5.60 Å.

Structure of [Ag₃(L3)(NH₃)₃]_n (7). X-ray structural analysis reveals that the asymmetric unit comprises of a fully deprotonated L3³⁻ trianion, three coordinated ammonia molecules, two crystallographically unique Ag(I) ions and two Ag(I) ions located in different inversion centers (Figure 7a). Ag1 and Ag3 ions exhibit standard linear geometry, Ag2 ion is almost linear geometry with N–Ag–O angle of 172.3(2)°. Ag4 ion exhibits T-shaped geometry. As observed in the aforementioned complexes, the argentophilic interactions are also found in complex **7** with the Ag \cdots Ag distances of 3.0920(11) Å (Ag1 \cdots Ag2), 2.9918(15) Å (Ag4 \cdots Ag4^{iv}), and 2.8094(8) Å (Ag3 \cdots Ag4), which make the present complex a novel structure with unique features. As shown in Figure 7b, the strong interactions between Ag3 and Ag4 extend the silver(I) ions into 1-D silver chains, which are further bridged by

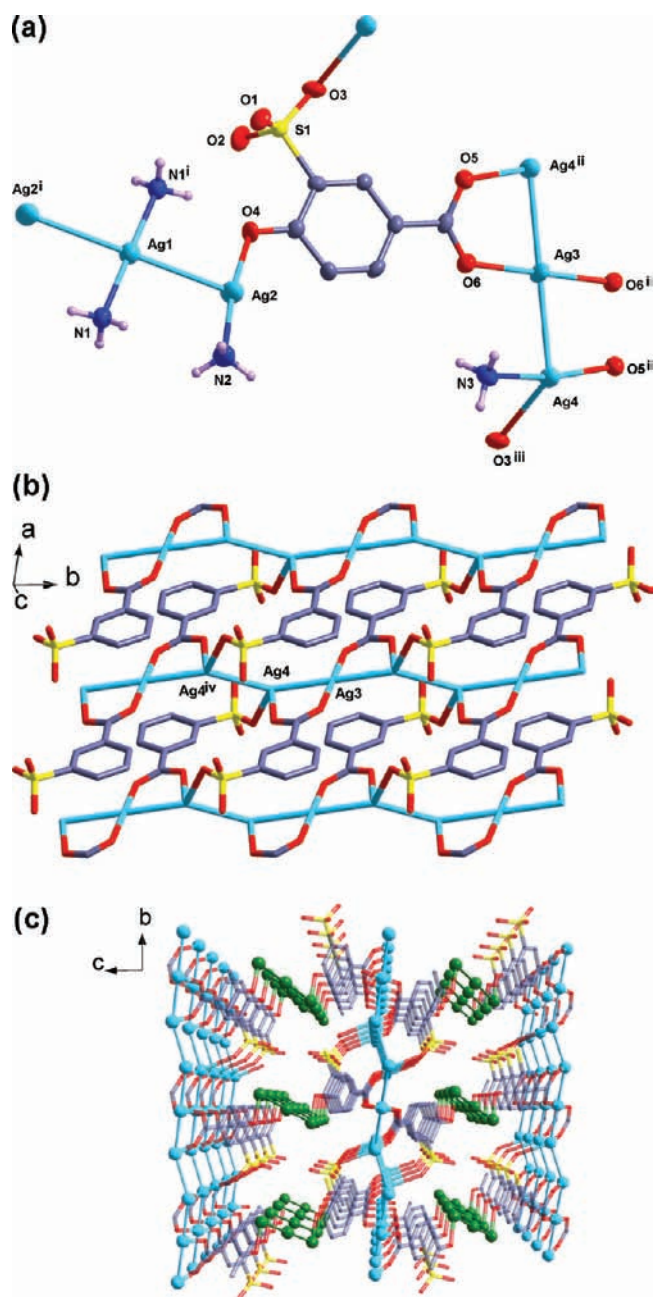


Figure 7. (a) Perspective view of the asymmetric unit of **7** showing the coordination environments around the silver centers with the ellipsoids drawn at the 50% probability level. (b) The Ag–O–S layer formed by the $L3^-$ trianions linking silver chains. (c) 3-D hybrid framework formed by the interlinked short triatom sticks and silver chains.

monodentate sulfonate group and bridging carboxylate group to construct 2-D layer. By contrast, adjacent Ag1 and Ag2 ions are linked by weak Ag \cdots Ag interactions into short triatom sticks. Subsequently, adjacent layers are linked by the short triatom sticks through hydroxyl groups of $L3^-$ trianions to afford the 3-D hybrid framework as illustrated in Figure 7c.

Structure of $[Ag_2(HL3)]_n$ (8**).** Complex **8** is 3D pillared layered framework with the asymmetric unit composed of two crystallographically unique Ag(I) ions and one $HL3^{2-}$ dianion (Figure 8a). Ag1 locates in a tetrahedron sphere, while Ag2 displays trigonal bipyramid geometry. Adjacent Ag(I) ions are bridged by the μ_2 mode of sulfonate O1 atom and unusual

μ_3 mode of carboxylate O5 atom as observed in complex **6** to generate interval eight-membered ring and three conterminous four-membered rings. It should be noted that the argentophilic interactions are found among the Ag(I) ions in the eight-membered ring with a longer distance of 3.3419(13) Å (Ag1 \cdots Ag2 iv) and a shorter distance of 2.7768(9) Å (Ag1 \cdots Ag1 iv). The assembly of these rings generates an infinite 1-D Ag–O tape along the crystallographic *a*-axis (Figure 8b). From another point of view, the 1-D tape can be described as dinuclears of edge-sharing Ag2 polyhedra interlinked by discrete Ag1 polyhedra by sharing vertexes and edges. Subsequently, the tetrahedrons of the sulfonates (CSO_3) link adjacent 1-D Ag–O tapes into 2-D infinite inorganic network substructure as illustrated in Figure 8c. Figure 8d exhibits the 3-D pillared layered framework of complex **8**, in which the phenyl rings act as the pillars. The gallery height of 4.78 Å (interlayer distance, 9.10 Å, the thickness of a single lamella, 4.32 Å) is shorter than that of complex **6**, which probably caused by the incline of the phenyl rings to the single lamella and subsequently shorten the distance between the adjacent layers.

Structure of $[Ag_6(L3)_2(H_2O)_3]_n$ (9**).** The molecular structure of complex **9** is shown in Figure 9a, Ag1 and Ag2 ions exhibit T-shaped geometry, while Ag3 and Ag4 ions exist in pseudotrigonal bipyramid geometry containing one carbon–carbon π interaction from η^2 -benzene of the sulfonate. The Ag–C distances for the two different ligands are unequal, being 2.404(8) and 2.559(8) Å for C6 and C7, 2.382(8) and 2.443(8) Å for C13 and C14, respectively, which well lie in the limits from 2.337 to 3.069 Å observed in the reported silver(I)–aromatic complexes,¹⁷ and indicate the existence of the strong Ag–C interactions. Ag5 ion has a tetrahedral geometry, while Ag6 ion, occupying 50% of the silver sites, presents linear geometry. The geometry of Ag7 ion can be described as trigonal bipyramidal geometry. Interestingly, it should be noted that ligand-supported argentophilic interactions can be observed between adjacent Ag(I) ions with various Ag \cdots Ag separations: (i) Ag1 \cdots Ag1 i (2.8511(18) Å); (ii) Ag1 \cdots Ag2 (3.3585(19) Å); (iii) Ag3 \cdots Ag4 (3.1339(10) Å); (iv) Ag5 \cdots Ag6 (2.8922(8) Å). These strong and weak Ag \cdots Ag interactions¹⁵ lead to the coexistence of dinuclear unit of $[Ag_3Ag_4]$, trinuclear unit of $[(Ag_5)_2Ag_6]$ and tetranuclear unit of $[Ag_1Ag_2]_2$. To the best of our knowledge, such various motifs are not detected in reported silver(I)–sulfonates.

Different from complexes **7** and **8**, the fully deprotonated $L3^{3-}$ trianion in complex **9** exhibits two types of intricate and novel coordination modes, namely, $\mu_{10}\text{-}\eta^5(SO_3H)$: $\eta^3(OH)$: $\eta^3(COOH)$: $\eta^2(C=C)$ and $\mu_8\text{-}\eta^4(SO_3H)$: $\eta^3(OH)$: $\eta^2(COOH)$: $\eta^2(C=C)$ (Scheme 1). In contrast to the two reported silver(I)–sulfonates involving a similar ligand H_3SSA ,^{4e,f,5a} the present coordination modes show unprecedented features. First, the μ_3 -bridging mode of the deprotonated hydroxyl group enriches the coordination fashion of $L3^{3-}$ group and coordination sphere of Ag(I) ion; Second, the strong Ag–C interactions are observed in rarely reported silver(I)–sulfonates;^{4c,7a} Third, assistance of the hydroxyl group intensifies the coordination ability of the so-called “weak” $-SO_3$ group and subsequently enriches the coordination fashion of $-SO_3$ group. As we reported in our previous work,^{6a} the O3 atom of the $-SO_3$ (S1) group exhibits rare κ^3 coordination mode,^{4c} whereas Shimizu has stated that the oxygen atoms of a $-SO_3$ group will bridge a maximum to two metal ions more typically.^{10b}

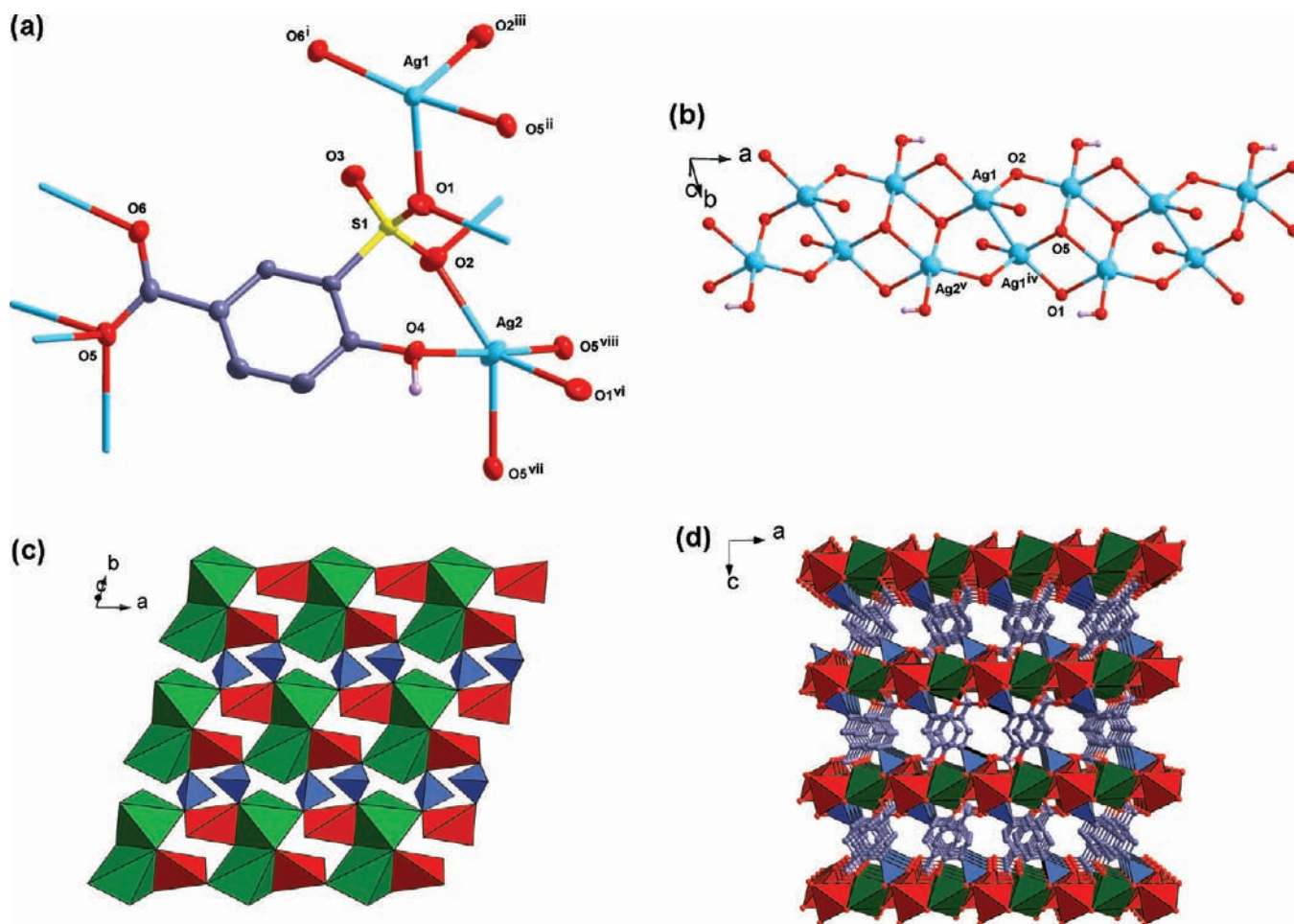


Figure 8. (a) Perspective view of the asymmetric unit of **8** showing the coordination environments around the silver centers with the ellipsoids drawn at the 50% probability level. (b) Infinite 1-D Ag–O tape with the Ag⋯Ag interactions denoted by sky blue solid line. (c) Polyhedral representation of the Ag–O–S layer (red polyhedra, Ag1; green polyhedra, Ag2; blue polyhedra, sulfonate group). (d) Illustration of the 3-D pillared layered structure.

From the above statement, the most remarkable feature of complex **9** is the four kinds of coordination spheres with low coordination number of two to five. As shown in Figure 9b, twelve polyhedra of Ag1, Ag2, Ag3, Ag4, Ag5, and Ag7 interconnected with each other by sharing vertexes and edges to form a dodecanuclear subunit, which are further linked to adjacent dodecanuclear subunits and Ag6 linear sticks through strongly argentophilic interactions between two adjacent Ag1 ions and Ag5, Ag6 ions to generate the inorganic lamellar network extending in the *ab* plane. Moreover, the pillars of $L3^{3-}$ groups bridge the adjacent layers to afford the 3-D pillared layered framework (Figure 9c). The difference of 6.26 Å between the interlayer distance (9.61 Å) and the thickness of a single lamella (3.35 Å) constitutes the gallery height, which is obviously shorter than that of $[Ag_4(HSSA)_2(H_2O)_2]_n$ (16.24 Å).^{4e,f,5a} The remarkable decrease of galley height may be attribute to the distinct coordination modes of the ligands. Furthermore, in our previous work, we presented the first silver-MPF of $[Ag_5(4\text{-pyridone-3-sulfonate})_3(NO_3)_2(H_2O)]_n$ (**HLJU-1**) which contains continuous silver(I) polyhedra with the higher coordination numbers of five to eight.^{6a} By contrast, complex **9** represents another silver(I)–MPF containing four kinds of coordination spheres with low coordination number of two to five. This result also indicates that all the coordination

spheres of Ag(I) ion with coordination numbers two to eight could afford the formation of silver(I)–MPFs.

Influencing Factor of the Structural Evolutions. It can be concluded from the aforementioned structural descriptions that the overall topological structures and the coordination spheres of Ag(I) ions of complexes **1–9** present intriguing variations (Figure S2 in Supporting Information). The structural evolutions are influenced by the synthetic methods, coordination modes and different benzenesulfonic acid ligands decorated by hydroxyl and carboxyl groups.

As illustrated in Chart 1, during the synthetic process with $AgNO_3$ and three benzenesulfonic ligands, two 0-D structures of **1**, **4** and two 3-D frameworks of **2**, **7** were obtained by adjusting the pH value to ~6 and 7–8 with proper amount of ammonia, respectively. In most cases, 0-D structures are more easier to be form in the above system owing to the strong affinity of ammonia to Ag(I) ion. However, the increasing of pH value and the formation of the additional Ag–Br and Ag⋯Ag interactions in complexes **2** and **7** afford two 3-D frameworks. Changed the metal salt into Ag_2CO_3 , one 2-D layer of **3** and four 3-D networks of **5**, **6**, **8**, and **9** with the corresponding benzenesulfonic ligands were obtained. In other words, the avoidance of ammonia could supply more coordinating space for the weak sulfonates to Ag(I) centers, thus effectively modulating the topological architectures and

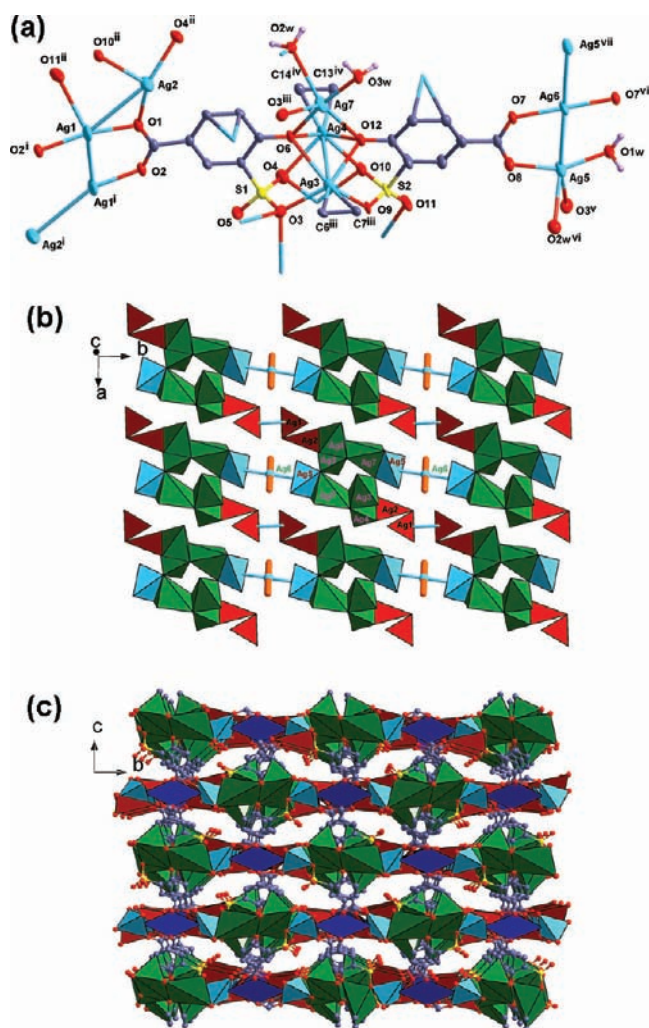


Figure 9. (a) Perspective view of the asymmetric unit of **9** showing the coordination environments around the silver centers with the ellipsoids drawn at the 50% probability level; the Ag...Ag interactions denoted by sky blue solid line. (b) Perspective view of the inorganic lamellar network, showing the different polyhedra of Ag(I) ions (orange stick denoted the linear coordination geometry of Ag6). (c) Illustration of the 3-D hybrid framework.

leading to high-dimensional structures. The formation of these complexes clearly demonstrates that the strong affinity of ammonia molecules and the N-heterocyclic ligands to Ag(I) ions is more preferable to afford the formation of linear unit —N—Ag—N— , which consequently prevents the coordination of sulfonates and induces the formation of low-dimensional structures.

In a more elaborate analysis, the form (deprotonated or not) and coordination behavior of the *ortho*-hydroxyl groups directly affect the coordination modes of the sulfonate groups, which subsequently generate different networks together with the multiple coordinating carboxyl groups. The hydroxyl group, when remains the H atom, exhibits three states, namely, uncoordinated (complexes **1**, **2**, and **4**), monodentate (complexes **2**, **3**, **6**, and **8**) and μ_2 -bridging (complex **5**) modes. Whereas the deprotonated hydroxyl group exhibits common monodentate (complex **7**) and rare μ_3 -bridging mode (complex **9**) as observed in our previous work.⁶ With the change of hydroxyl group, the sulfonate group exhibits diverse coordination modes, which determines the dimension of the

complexes with the assistant of carboxyl groups. In complexes **1** and **4**, the sulfonate groups exhibit uncoordinated and simple monodentate modes, while the carboxyl groups exhibit monodentate and bridging modes, respectively. Accordingly, such simple coordination modes and the terminal coordination of ammonia lead to the formation of two 0-D complexes. The sulfonate groups in complexes **2** and **3** exhibit μ_2 ($\kappa^1\text{O}:\kappa^1\text{O}$) and μ_4 ($\kappa^2\text{O}:\kappa^1\text{O}:\kappa^1\text{O}$) modes, whereas the carboxyl groups exhibit the same bridging mode. However, complex **2** presents 3-D framework with the connection of Ag—Br bonds in contrast to complex **3**. The monodentate mode of hydroxyl groups in complexes **6** and **8** makes the sulfonate groups exhibit the same μ_4 ($\kappa^2\text{O}:\kappa^2\text{O}$) fashions, which connect adjacent Ag(I) ions to give rise to 1-D concave–convex chain (complex **6**) and 1-D tape (complex **8**). The carboxyl groups, with rarely μ_4 ($\kappa^1\text{O}:\kappa^3\text{O}$) mode, link the aforementioned chains into 3-D pillared layered frameworks. Different from the above six complexes, the hydroxyl group in complex **5** exhibits μ_2 -bridging mode and connects adjacent Ag(I) ions with μ_3 -bridging ($\kappa^2\text{O}:\kappa^1\text{O}$) sulfonate group and monodentate carboxyl group to generate 3-D framework. Although the hydroxyl group in complex **7** is deprotonated, the sulfonate group only exhibits the simplest monodentate mode. Fortunately, the bridging carboxyl group and the Ag...Ag interactions extend complex **7** into 3-D frameworks. By contrast, the deprotonated hydroxyl group in complex **9** exhibit interesting μ_3 -bridging mode as reported in previous work.⁶ Simultaneously, the sulfonate groups act in μ_4 ($\kappa^2\text{O}:\kappa^2\text{O}$) and μ_4 ($\kappa^2\text{O}:\kappa^1\text{O}:\kappa^1\text{O}$) modes, while the carboxyl groups act in bridging and μ_3 ($\kappa^2\text{O}:\kappa^1\text{O}$) modes. These intricate coordination modes of the three functional groups result in the formation of 3-D pillared layered frameworks.

On the basis of the above description, the hydroxyl and carboxyl group-substituted benzenesulfonic acids are excellent bridging ligands, which can be used to construct 3-D frameworks. Moreover, the acquirement of complex **9** further demonstrate the conclusion that deprotonated hydroxyl group can form novel μ_3 -bridging mode and result in complicated coordination modes of sulfonate group, which, in turn, create the large tendency to form high dimensional frameworks. Importantly, the carboxyl groups in the nine complexes present four types of coordination modes, namely, μ_1 ($\kappa^1\text{O}$), μ_2 ($\kappa^1\text{O}:\kappa^1\text{O}$), μ_3 ($\kappa^2\text{O}:\kappa^1\text{O}$), and μ_4 ($\kappa^1\text{O}:\kappa^3\text{O}$), which indicates that the carboxyl group possesses strong coordination ability in comparison with the hydroxyl and sulfonate groups. The μ_2 to μ_4 mode play crucial role in the construction of high-dimensional networks. Especially, the μ_4 ($\kappa^1\text{O}:\kappa^3\text{O}$) fashion in complexes **6** and **8** is rarely observed in the reported silver(I)–carboxylates.¹²

IR Spectroscopy. The peaks observed at the range of $1617\text{--}1583\text{ cm}^{-1}$ for complexes **1–4** and **6–9** are assigned to the stretching bands of $\nu_{\text{as}}(\text{COO}^-)$, while the peaks observed at the range of $1427\text{--}1369\text{ cm}^{-1}$ can be assigned to the stretching bands of $\nu_{\text{s}}(\text{COO}^-)$. The observations of these peaks indicate that the carboxyl groups in complexes **1–4** and **6–9** are deprotonated and coordinate to the Ag(I) ion in diverse coordination modes.¹⁸ By contrast, the peak at 1688 cm^{-1} for complex **5** can be attributed to the vibration of C=O , which demonstrates that the H atom of the carboxyl group is not removed. The characteristic vibrations of $\nu_{\text{as}}(\text{SO}_3^-)$ in complexes **1–9** are at the range of $1268\text{--}1119\text{ cm}^{-1}$, whereas the $\nu_{\text{s}}(\text{SO}_3^-)$ absorptions are at the range of $1037\text{--}1010\text{ cm}^{-1}$. In addition, the IR spectra of complexes **1–9** exhibit strong and

Scheme 1. Coordination Modes of the Three Arenesulfonate Ligands in Complexes 1–9

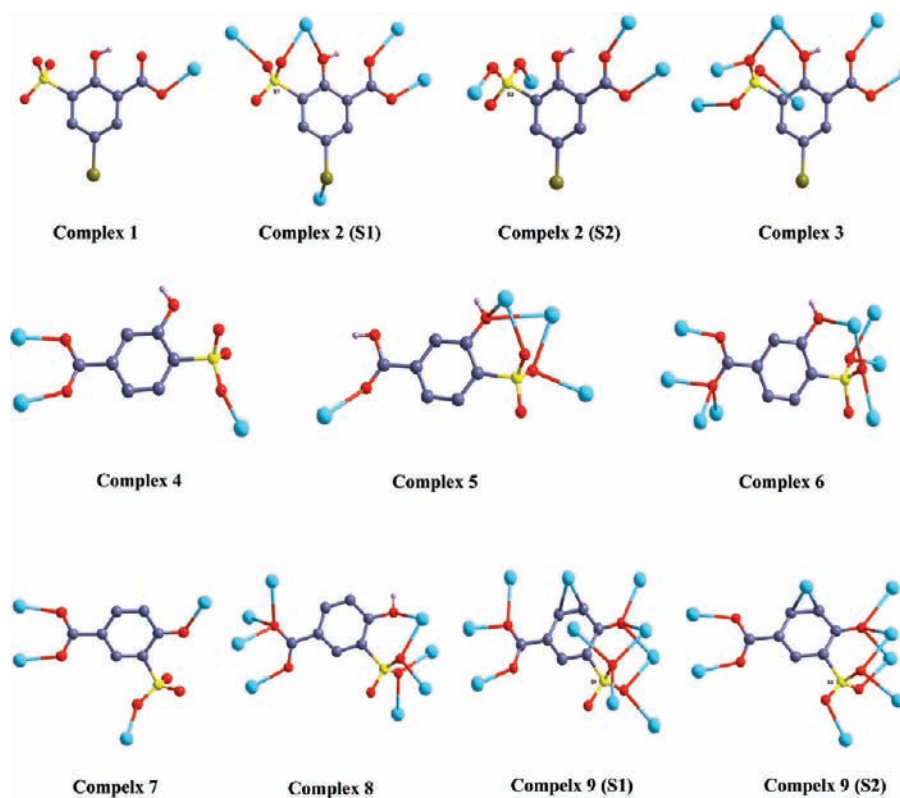
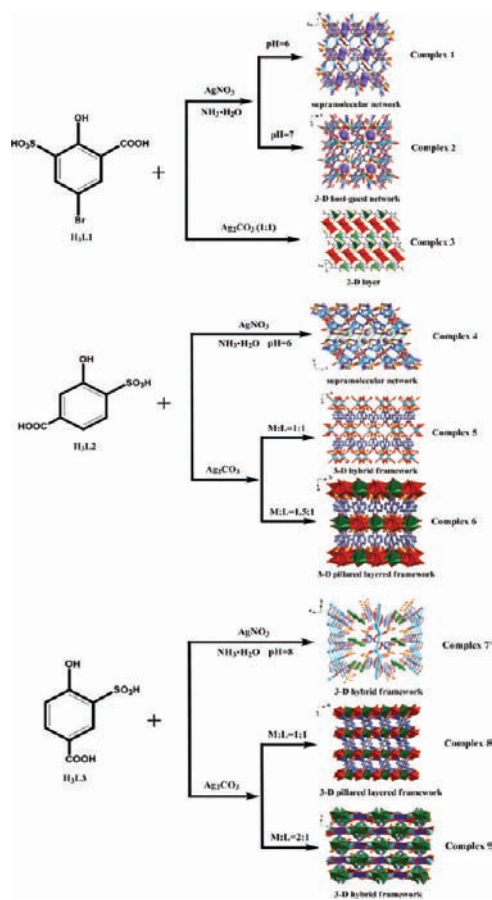


Chart 1. Representation of the Synthetic Process of Complexes 1–9



broad absorptions in the range of $3480\text{--}3178\text{ cm}^{-1}$, occurring because of the existence of hydrogen bonds formed by water molecules, ammonia molecules, ammonium cations, as well as the hydroxyl groups in the nine complexes.

Luminescent Property. Complexes with d^{10} metal centers and organic ligands are promising candidates for photoluminescent materials.¹⁹ The luminescent properties of complexes 1–9 and three free ligands in the solid-state at room temperature were investigated. Upon excitation at 328, 280, and 313 nm, free ligands $\text{H}_3\text{L1}$ – $\text{H}_3\text{L3}$ exhibit emission maximum at 456, 353, and 437 nm, which is probably attribute to the intraligand transitions (Figure 10 and Figure S3 in Supporting Information). Unfortunately, no obvious emissions for complexes 4 and 6–9 were detected. As shown in Figure 10a and Figure 10b, upon excitation at 339 nm, complexes 1–3 exhibit blue emission maximum at 442, 434, and 438 nm, while complex 5 exhibits purple blue emission maximum at 369 nm upon excitation at 328 nm (for Luminescent photographs of the four complexes, see Figure S4 in Supporting Information). These fluorescent emission bands can probably be assigned to the intraligand (IL) $\pi\text{--}\pi^*$ transitions because the resemblance of the emission spectra in comparison with free ligands $\text{H}_3\text{L1}$ and $\text{H}_3\text{L2}$.^{7b,20} The blue shifts of the emission peaks in complexes 1–3 and red shift of the emission peak in complex 5 are probably attributable to the differences of ligands and the coordination environment around Ag(I) ions.²¹

Owing to the strong emission and well solubility in aqueous solution, complex 1 was selected to investigate its luminescent behavior. An attractive luminescent feature of complex 1 is the sensitization to lanthanide. Usually, Eu(III) and Tb(III) ions cannot exhibit characteristic emission at room temperature in aqueous solution. However, it is interesting to note that the addition of the same equivalent of complex 1 into the aqueous

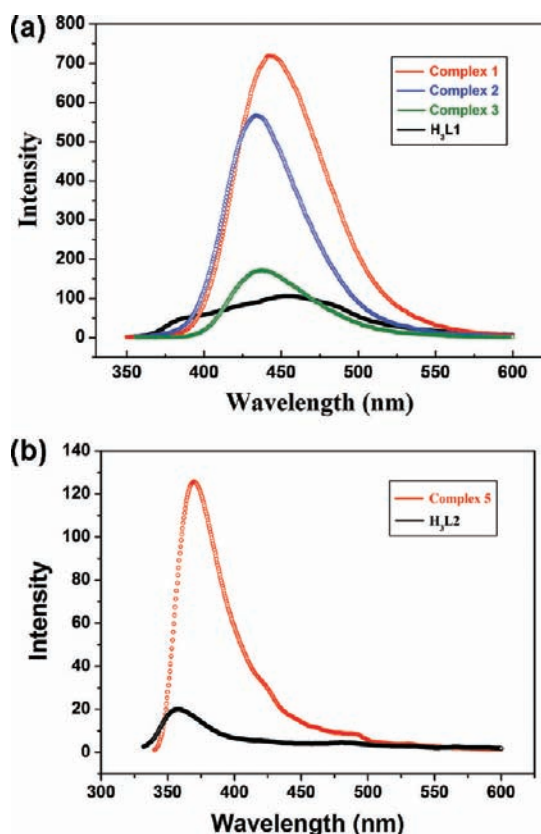


Figure 10. (a) Emission spectra of complexes 1–3 and ligand H_3L1 in the solid-state at room temperature. (b) Emission spectrum of complex 5 and ligand H_3L2 in the solid-state at room temperature.

solution makes the Tb(III) ion exhibit the characteristic transition of $^5D_4 \rightarrow ^7F_J$ ($J = 3-6$) (Figure 11). But in the

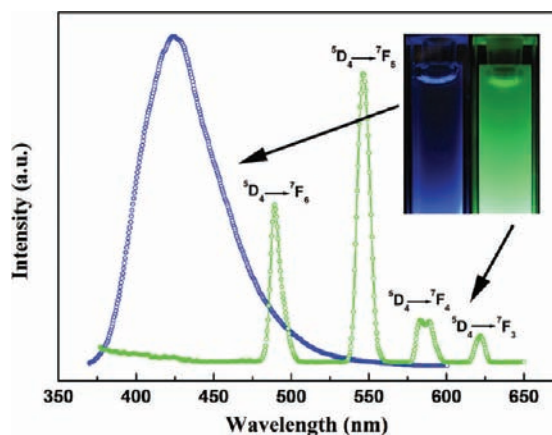


Figure 11. Emission spectra of complex 1 upon addition of 1×10^{-4} mol·L $^{-1}$ of $Tb(NO_3)_3$ in aqueous solution. Inset: Photographs of complex 1 in aqueous solution and after addition of 1×10^{-4} mol·L $^{-1}$ of $Tb(NO_3)_3$.

aqueous solution containing equal amount of Eu(III) ion and complex 1, the luminescence characteristic emission wavelengths of the Eu(III) ion were not observed. It is well-known that the luminescence of Ln(III) is related to the efficiency of the energy transfer from the triplet state of the ligand to the emitting level of the Ln(III) ions, which depends on the energy gap between the two levels.²² In Tb(III) ion containing

solution, the energy gap between the ligand triplet state and the emitting level of the Tb(III) ion may be in favor of the energy transfer process. Whereas the energy gap between the ligand triplet state and the emitting level of the Eu(III) ion was not in favor of the energy transfer process and thus no obvious characteristic emissions of Eu(III) ion was observed. Although the mechanism for sensitization to Tb(III) ion is still not clear at this moment, the replacement of Ag(I) ion by Tb(III) ion and the coordination of the free functional groups to the Tb(III) ion definitely play an important role. Moreover, the luminescent properties of complex 1 in different solvents and different pH values in aqueous solution were also investigated due to the solubility in different solvents. (Figure S5 and S6 in Supporting Information).

CONCLUSIONS

In summary, self-assembly of silver(I) salts and three benzenesulfonic acids decorated by hydroxyl and carboxyl groups leads to the formation of a new family of silver(I)-sulfonates with two 0-D discrete motifs, one 2-D layer, and six 3-D frameworks. The structural diversities and evolutions can be attributed to the synthetic methods, different ligands and coordination modes of the three functional groups. Luminescent investigations indicate that complexes 1–3 and 5 exhibit strong blue emissions at room temperature. Moreover, it is interesting to note that complex 1 can sensitize Tb(III) ion to exhibit characteristic emissions at room temperature in aqueous solution.

This study clearly demonstrates that the attachment of carboxyl and hydroxyl groups to the benzenesulfonic acid can effectively bridge more metal centers to construct 3-D frameworks. This result must promote the development of crystal engineering and coordination chemistry of metal-sulfonates. Bear these results in mind, further syntheses, structures and properties studies of high-dimensional silver(I)-sulfonates with multiple functional arenesulfonic acids are also underway in our laboratory.

ASSOCIATED CONTENT

Supporting Information

Additional figures, luminescent behavior of complex 1, TG analyses, selected bond distances and angles, and selected hydrogen bond parameters for all complexes, as well as the X-ray crystallographic files in CIF format. This material is available free of charge via the Internet at <http://pubs.acs.org>.

ACKNOWLEDGMENTS

This work is financial supported by the Key Project of Natural Science Foundation of Heilongjiang Province (No. ZD200903), Key Project of Education Bureau of Heilongjiang Province (No. 12511z023, No. 2011CJHB006), and the Innovation team of Education bureau of Heilongjiang Province (No. 2010td03). We thank the University of Heilongjiang (Hdtd2010-04, yjscx2010-015hju) for supporting this study. Special thanks are offered to Xin-Lei Li, a student of Fuzhou No. 19 Middle School in Fujian China, for the drawing of the two cartoons in the TOC picture.

REFERENCES

- (1) (a) Li, F.-F.; Ma, J.-F.; Song, S.-Y.; Yang, J.; Liu, Y.-Y.; Su, Z.-M. *Inorg. Chem.* **2005**, *44*, 9374. (b) Li, F.-F.; Ma, J.-F.; Song, S.-Y.; Yang, J. *Cryst. Growth Des.* **2006**, *6*, 209. (c) Lian, Z.-X.; Cai, J.; Chen, C.-H.; Luo, H.-B. *CrystEngComm* **2007**, *9*, 319. (d) Liu, H.-Y.; Wu, H.;

- Ma, J.-F.; Song, S.-Y.; Yang, J.; Liu, Y.-Y.; Su, Z.-M. *Inorg. Chem.* **2007**, *46*, 7299. (e) Wang, Y.-L.; Liu, Q.-Y.; Xu, L. *CrystEngComm* **2008**, *10*, 1667. (f) Wu, H.; Dong, X.-W.; Liu, H.-Y.; Ma, J.-F.; Li, S.-L.; Yang, J.; Liu, Y.-Y.; Su, Z.-M. *Dalton Trans.* **2008**, 5331. (g) Wu, H.; Dong, X.-W.; Ma, J.-F.; Liu, H.-Y.; Yang, J.; Bai, H.-Y. *Dalton Trans.* **2009**, 3162. (h) Liu, H.-Y.; Wu, H.; Ma, J.-F.; Yang, J.; Liu, Y.-Y. *Dalton Trans.* **2009**, 7957. (i) Xiong, K.; Wu, M.; Zhang, Q.; Wei, W.; Yang, M.; Jiang, F.; Hong, M. *Chem. Commun.* **2009**, 1840. (j) Yeh, C.-W.; Chen, T.-R.; Chen, J.-D.; Wang, J.-C. *Cryst. Growth Des.* **2009**, *9*, 2595. (k) Li, C.-P.; Chen, J.; Yu, Q.; Du, M. *Cryst. Growth Des.* **2010**, *10*, 1623.
- (2) (a) Downer, S. M.; Squatrito, P. J.; Bestaoui, N.; Clearfield, A. J. *Chem. Cryst.* **2006**, *36*, 487. (b) Wu, H.; Dong, X.-W.; Ma, J.-F. *Acta Crystallogr.* **2006**, *E62*, m385. (c) Liu, H.-Y.; Wu, H.; Ma, J.-F. *Acta Crystallogr.* **2006**, *E62*, m1036.
- (3) Shimizu, G. K. H.; Enright, G. D.; Rego, G. S.; Ripmeester, J. A. *Can. J. Chem.* **1999**, *77*, 313.
- (4) (a) Shimizu, G. K. H.; Enright, G. D.; Ratcliffe, C. I.; Rego, G. S.; Reid, J. L.; Ripmeester, J. A. *Chem. Mater.* **1998**, *10*, 3282. (b) Shimizu, G. K. H.; Enright, G. D.; Preston, K. F.; Ratcliffe, C. I.; Reid, J. L.; Ripmeester, J. A. *Chem. Commun.* **1999**, 1485. (c) Côté, A. P.; Shimizu, G. K. H. *Inorg. Chem.* **2004**, *43*, 6663. (d) May, L. J.; Shimizu, G. K. H. *Chem. Mater.* **2005**, *17*, 217. (e) Ma, J.-F.; Yang, J.; Li, S.-L.; Song, S.-Y.; Zhang, H.-J.; Wang, H.-S.; Yang, K.-Y. *Cryst. Growth Des.* **2005**, *5*, 807. (f) Gao, S.; Zhu, Z.-B.; Huo, L.-H.; Ng, S. W. *Acta Crystallogr.* **2005**, *E61*, m279. (g) Gao, S.; Lu, Z.-Z.; Huo, L.-H.; Zhu, Z.-B.; Zhao, H. *Acta Crystallogr.* **2005**, *C61*, m22. (h) Akhbari, K.; Morsali, A.; Rafiei, S.; Matthias, Z. *J. Organomet. Chem.* **2008**, *693*, 257. (i) Prochniak, G.; Videnova-Adrabska, V.; Daszkiewicz, M.; Pietraszko, A. *J. Mol. Struct.* **2008**, *891*, 178.
- (5) (a) Gao, S.; Zhu, Z.-B.; Huo, L.-H.; Ng, S. W. *Acta Crystallogr.* **2005**, *E61*, m282. (b) Hoffart, D. J.; Dalrymple, S. A.; Shimizu, G. K. H. *Inorg. Chem.* **2005**, *44*, 8868. (c) Lü, J.; Gao, S.-Y.; Lin, J.-X.; Shi, L.-X.; Cao, R.; Batten, S. R. *Dalton Trans.* **2009**, 1944.
- (6) (a) Deng, Z.-P.; Zhu, Z.-B.; Gao, S.; Huo, L.-H.; Zhao, H. *Dalton Trans.* **2009**, 1290. (b) Deng, Z.-P.; Zhu, Z.-B.; Gao, S.; Huo, L.-H.; Zhao, H.; Ng, S. W. *Dalton Trans.* **2009**, 6552.
- (7) (a) Deng, Z.-P.; Li, M.-S.; Zhu, Z.-B.; Huo, L.-H.; Zhao, H.; Gao, S. *Organometallics* **2011**, *30*, 1961. (b) Deng, Z.-P.; Huo, L.-H.; Li, M.-S.; Zhang, L.-W.; Zhu, Z.-B.; Zhao, H.; Gao, S. *Cryst. Growth Des.* **2011**, *11*, 3090.
- (8) (a) Venkataraman, D.; Du, Y.; Wilson, S. R.; Zhang, P.; Hirsch, K.; Moore, J. S. *J. Chem. Educ.* **1997**, *74*, 915. (b) Khlobystov, A. N.; Blake, A. J.; Champness, N. R.; Lemenovskii, D. A.; Majouga, A. G.; Zyk, N. V.; Schröder, M. *Coord. Chem. Rev.* **2001**, *222*, 155. (c) Zheng, S.-L.; Tong, M.-L.; Chen, X.-M. *Coord. Chem. Rev.* **2003**, *246*, 185. (d) Chen, C.-L.; Kang, B.-S.; Su, C.-Y. *Aust. J. Chem.* **2006**, *59*, 3. (e) Steel, P. T.; Fitchett, C. M. *Coord. Chem. Rev.* **2008**, *252*, 990. (f) Young, A. G.; Hanton, L. R. *Coord. Chem. Rev.* **2008**, *252*, 1346.
- (9) (a) Côté, A. P.; Shimizu, G. K. H. *Chem.—Eur. J.* **2003**, *9*, 5361. (b) Makinen, S. K.; Melcer, N. J.; Parvez, M.; Shimizu, G. K. H. *Chem.—Eur. J.* **2001**, *7*, 5176.
- (10) (a) Côté, A. P.; Shimizu, G. K. H. *Coord. Chem. Rev.* **2003**, *245*, 49. (b) Shimizu, G. K. H.; Vaidhyanathan, R.; Taylor, J. M. *Chem. Soc. Rev.* **2009**, *38*, 1430.
- (11) Cambridge Structure Database search, CSD Version 5.27 (November 2005) with 16 updates (January 2006–Feb 2011).
- (12) (a) Jiang, X.-J.; Zhang, S.-Z.; Guo, J.-H.; Wang, X.-G.; Li, J.-S.; Du, M. *CrystEngComm* **2009**, *11*, 855. (b) Jin, J.; Niu, S.; Han, Q.; Chi, Y. *New J. Chem.* **2010**, *34*, 1176.
- (13) Sheldrick, G. M. *SHELXTL-97, Program for Crystal Structure Solution and Refinement*; University of Göttingen: Göttingen, Germany, 1997.
- (14) Stork, J. R.; Thoi, V. S.; Cohen, S. M. *Inorg. Chem.* **2007**, *46*, 11213.
- (15) (a) Bondi, A. J. *J. Phys. Chem.* **1964**, *68*, 441. (b) Deng, Z.-P.; Huo, L.-H.; Zhu, L.-N.; Zhao, H.; Gao, S. *Polyhedron* **2010**, *29*, 3207. (c) Black, C. A.; Hanton, L. R.; Spicer, M. D. *Inorg. Chem.* **2007**, *46*, 3669. (d) Zhou, X.-P.; Zhang, X.-J.; Lin, S.-H.; Li, D. *Cryst. Growth Des.* **2007**, *7*, 485. (e) Zang, S.-Q.; Mak, T. C. W. *Inorg. Chem.* **2008**, *47*, 7094.
- (16) (a) Charbonnier, F.; Faure, R.; Loiseau, H. *Acta Crystallogr.* **1978**, *B34*, 3598. (b) Laube, T.; Weidenhaupt, A.; Hunziker, R. *J. Am. Chem. Soc.* **1991**, *113*, 2561.
- (17) (a) Munakata, M.; Wu, L. P.; Kuroda-Sowa, T.; Maekawa, M.; Suenaga, Y.; Sugimoto, K. *Inorg. Chem.* **1997**, *36*, 4903. (b) Munakata, M.; Wu, L. P.; Kuroda-Sowa, T.; Maekawa, M.; Suenaga, Y.; Ning, G. L.; Kojima, T. *J. Am. Chem. Soc.* **1998**, *120*, 8610. (c) Ning, G. L.; Wu, L. P.; Sugimoto, K.; Munakata, M.; Kuroda-Sowa, T.; Maekawa, M. *J. Chem. Soc., Dalton Trans.* **1999**, 2529. (d) Zang, S.-Q.; Han, J.; Mak, T. C. W. *Organometallics* **2009**, *28*, 2677.
- (18) Nakakamoto, K. *Infrared and Raman of Inorganic and Coordination Compounds*, 4th ed.; John Wiley & Sons, Inc.: New York, 1986; pp 223.
- (19) (a) Wu, Q.; Esteghamatian, M.; Hu, N.-X.; Popovic, Z.; Enright, G.; Tao, Y.; D'Orio, M.; Wang, S. *Chem. Mater.* **2000**, *12*, 79. (b) McGarragh, J. E.; Kim, Y.-J.; Hissler, M.; Eisenberg, R. *Inorg. Chem.* **2001**, *40*, 4510. (c) Santis, G. D.; Fabbri, L.; Licchelli, M.; Poggi, A.; Taglietti, A. *Angew. Chem., Int. Ed.* **1996**, *35*, 202.
- (20) (a) Alcock, N. W.; Barker, P. R.; Haider, J. M.; Hannon, M. J.; Painting, C. L.; Pikramenon, Z.; Plummer, E. A.; Rissanen, K.; Saarenketo, P. *J. Chem. Soc., Dalton Trans.* **2000**, 1447. (b) Collin, J. P.; Dixon, I. M.; Sauvage, J. P.; Williams, J. A. G.; Barigelletti, F.; Flamigni, L. *J. Am. Chem. Soc.* **1999**, *121*, 5009. (c) Xiong, R.-G.; Zuo, J.-L.; You, X.-Z.; Fun, H.-K.; Raj, S. S. S. *Organometallics* **2000**, *19*, 4183.
- (21) Valeur, B. *Molecular Fluorescence: Principles and Applications*; Wiley-VCH: Weinheim, Germany, 2002.
- (22) (a) Arnaud, N.; Vaquer, E.; Georges, J. *Analyst* **1998**, *123*, 261. (b) Yang, X.; Jones, R. A. *J. Am. Chem. Soc.* **2005**, *127*, 7686.